# Transesterification of dimethyl carbonate with tetrahydrofurfuryl alcohol on the $K_2CO_3/ZrO_2$ catalyst—Function of the surface carboxylate species

Bin Zhang [a], Guoqiang Ding [b], Hongyan Zheng [b], Yulei Zhu [a,b,*]

[a] State Key Laboratory of Coal Conversion, Institute of Coal Chemistry, Chinese Academy of Sciences, PO Box 165, Taiyuan 030001, PR China
[b] Synfuels CHINA Co. Ltd, Taiyuan 030032, PR China

## ARTICLE INFO

## ABSTRACT

An efficient and selective synthesis of unsymmetrical tetrahydrofurfuryl carbonate and other organic carbonates was realized in the liquid phase transesterification dimethyl carbonate (DMC) with alcohols over the $K_2CO_3/ZrO_2$ catalyst. Compared with MgO, CaO, MgAl-HDT, $ZrO_2$, and $CsF/\alpha$-$Al_2O_3$, the $K_2CO_3/ZrO_2$ catalyst with lower basicity displayed a significantly higher activity. The results of FT-IR, XPS and $CO_2$-TPD suggested that the carboxylate species on the surface of the $K_2CO_3/ZrO_2$ catalyst were the active sites for the DMC transesterification. Other $K_2CO_3$ supported $TiO_2$, $SiO_2$ and $Al_2O_3$ catalysts showed a rather low catalytic activity due to the lack of carboxylate species.

© 2014 Elsevier B.V. All rights reserved.

## 1. Introduction

Biomass, the sustainable source of energy and organic carbon, has the potential to displace nonrenewable fossil resources in the production of chemicals and liquid transportation fuels [1,2]. The utilization of $CO_2$ as an attractive C1 building block and sustainable carbon resource, which has abundant amount as greenhouse compound, has also drawn much attention in recent years [3,4]. It is a new approach to achieve highly efficient reactions to meet the chemical economies and green chemistry in the utilization of these carbon resources. Organic carbonates have extensive applications, from fine chemicals, biological, and medicine to plasticizers, lubricants and solvents [5–8]. However, the toxic and hazardous phosgene was commonly used to synthesis of these compounds [4,9]. Recently, dimethyl carbonate (DMC), which can be synthesized from $CO_2$ [4,10], was regarded as an environmentally friendly green reagent to replace phosgene in several reactions, particularly in the production of organic carbonates [9,11]. However, the biomass derivative products of the DMC were less studied. The tetrahydrofurfuryl alcohol (THFA) is a

biomass-derived compounds, which can be converted into several important chemicals including dihydropyran or δ-hydroxyvaleraldehyde by acid-catalysis [12], and 1,5-pentanediol by hydrogenolysis [13]. THFA carbonate has a high oxygen content and boiling point, which make it to be more attractive oxygen containing fuel additive than DMC and methanol. However, few synthetic routes for THC have been described. Transesterification of DMC with THFA is an appropriate and attractive route for the synthesis of methyl tetrahydrofurfuryl carbonate (TMC) and bis(tetrahydrofurfuryl) carbonate (DTC) (Scheme 1).

The transesterification of DMC with alcohols is conventionally carried out in the liquid phase by using the homogeneous catalysts such as Sn, Ti, Al, and Fe organometallic compounds [14–17], and the heterogeneous catalysts such as $MoO_3/SiO_2$ [18], $TiO_2/SiO_2$ [19], and rare earth metal oxides [18,20]. However, the homogeneous catalysts are unstable and not easy to separate from the products, and the catalytic activity and selectivity are low over the heterogeneous catalysts. It is desirable to find more efficient and cheap heterogeneous catalysts for the transesterification of DMC with alcohol.

Recently, the basic Mg–Al-hydrotalcite (MgAl-HDT) catalyst showed a higher activity than conventional MgO, CaO, $Mo/SiO_2$ and $TiO_2/SiO_2$ catalysts in the transesterification of DMC with phenol [21] or glycerol [7]. However, it displayed a lower activity than the supported $NaOH/\gamma$-$Al_2O_3$ catalyst in the synthesis of glycerol carbonate from glycerol and DMC [22]. Nevertheless, the leaching of
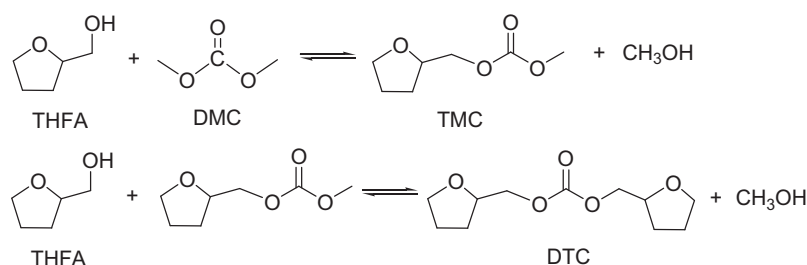
**Scheme 1.** The synthesis of tetrahydrofurfuryl alcohol carbonate from dimethyl carbonate and tetrahydrofurfuryl alcohol by transesterification.

ionic species (Na$^+$, OH$^-$) resulted in the activity loss of the NaOH/γ-Al$_2$O$_3$ catalyst. Similarly, the solubility of K$_2$CO$_3$ was decidedly high in polar solvents, thought the polyethylene glycol modified K$_2$CO$_3$ was more active than MgAl-HDT and ion-exchange resins (strongly acidic, superacidic, weakly acidic, basic) [23]. A strong interaction between the K$_2$CO$_3$, NaOH or other basic salts and the support can inhibit the salt erosion during the reaction. The Cs-ZrO$_2$ catalyst, prepared by cation exchange of zircomium hydroxide with CsCO$_3$, was reported to be a more effective solid base than MgAl-HDT and NaOH in vegetable oil transesterification [24]. Both the amount of the basic sites and superficial carbonates were significantly increased by the Cs promotion on the ZrO$_2$ support. But the function of the carbonates over the Cs-ZrO$_2$ catalyst was not discussed. Fan and Zhang have found that the supported K$_2$CO$_3$/AC (AC, active carbon) and KOH/AC catalyst showed higher activity in compared with KHCO$_3$/AC and K$_2$HPO$_4$/AC catalyst for the transesterification of DMC with propyl alcohol [25], and the carbonate anion (CO$_3^{2-}$) was considered as the active site without any further proof.

Herein we report a fast and selective synthesis of unsymmetrical organic carbonates including THC in the presence of a new, recyclable K$_2$CO$_3$/ZrO$_2$ solid catalyst via transesterification of DMC with various alcohols. The surface active sites were characterized. The effects of support in the generation of active sites were studied. The role of the carbonate species on the catalyst surface were measured and discussed.

## 2. Experimental

### 2.1. Catalyst preparation

The ZrO$_2$ support was prepared by co-precipitation method using the 0.5 M zirconium oxychloride aqueous solution and 1 M NH$_3$ aqueous solution at room temperature and pH 9. The precipitate was aged for 1 h, and them separated by filtration and washed with distilled water to remove the chloride ions. The obtained precipitate was dried in static air at 110 °C for 12 h followed by calcination at 600 °C for 5 h. The MgO and MgAl-HDT were also prepared by co-precipitation method using Na$_2$CO$_3$ (0.5 M) as precipitant. The α-Al$_2$O$_3$ was obtained by the calcinations of γ-Al$_2$O$_3$ ($S_{BET}$ = 197 m$^2$/g, Shandong Aluminum Co., Ltd., China) at 1200 °C for 5 h.

The K$_2$CO$_3$/ZrO$_2$ catalyst was prepared by incipient wetness impregnation of ZrO$_2$ with an aqueous solution of K$_2$CO$_3$ (Sinopharm Chemical Reagent Co., Ltd, China) for 24 h. After that, the resulting powders were dried at 110 °C overnight, and then calcined in air at 600 °C for 5 h. The same method was used in the preparation of K$_2$CO$_3$/TiO$_2$, K$_2$CO$_3$/CeO$_2$, K$_2$CO$_3$/γ-Al$_2$O$_3$, K$_2$CO$_3$/α-Al$_2$O$_3$ and K$_2$CO$_3$/SiO$_2$, using TiO$_2$ (99.9% anatase, $S_{BET}$ = 149 m$^2$/g, Nanjing High Technology Nano Material Co., Ltd.), CeO$_2$ ($S_{BET}$ = 80.3 m$^2$/g) and γ-Al$_2$O$_3$, α-Al$_2$O$_3$ and SiO$_2$ (Qingdao Haiyang Co. Ltd., $S_{BET}$ = 393.0 m$^2$/g) as supports, respectively. Other catalysts, such as CsF/α-Al$_2$O$_3$, KNO$_3$/ZrO$_2$, KNO$_3$/γ-Al$_2$O$_3$, were

also prepared via the incipient wetness impregnation method. The content of K or Cs in all the supported catalysts was 1 mmol/g, which was measured by ICP-AES.

### 2.2. Catalyst characterization

The textural characterization of the catalysts was based on the nitrogen adsorption isotherm, determined at the normal boiling point of N$_2$ (−196 °C) with a Micromeritics ASAP 2500 instruments. Each sample was degassed under vacuum at 90 °C for 1 h and 350 °C for 8 h prior to the measurement.

Powder X-ray diffraction (XRD) patterns of the samples were measured on a D/max-RA X-ray diffractometer (Rigaku, Japan) with Cu Kα radiation (λ = 0.154 nm) operated at 40 kV and 100 mA.

Temperature-programmed desorption (TPD) of carbon dioxide was performed using an Auto chem. II 2920 equipment (Micromeritics, USA). The samples were first activated at 500 °C for 1 h and subsequently cooled to 50 °C under a helium flow. The activated materials were then saturated with dry gaseous carbon dioxide (99.999%) at the same temperature. When the adsorption finished, the sample was purged with a helium flow and then the CO$_2$-TPD performed at a rate of 10 °C/min to 700 °C.

FTIR study of the catalyst was performed on an infrared spectrometer (VEREX70, Bruker, Germany), using the KBr pellet technique.

X-ray photoelectron spectra (XPS) were recorded with a VG MiltiLab 2000 system (VG) at a base pressure of $1 \times 10^{-9}$ mbar. Samples were excited with monochromatized Mg Kα radiation ($h\nu$ = 1253.6 eV). The analyzer was operated in a constant-pass energy mode (20 eV). The C1s peak of adventitious carbon (284.6 eV) was used as a reference for estimating the binding energy. The binding energies are given with an accuracy of ±0.1 eV.

### 2.3. Activity test and analysis method

Catalytic tests were performed in a 100 mL stainless steel autoclave at a stirring speed of 600 rpm. In a typical run, an excess of DMC (0.32 mol), 0.01 mol THFA (Sinopharm Chemical Reagent Co., Ltd) and 0.01 g catalyst were introduced into the autoclave. Afterwards, the reactor was purged with N$_2$ three times and then heated to 130 °C. Stirring was continued until the completion of the reaction. The experiments were rapidly stopped using an ice-bath to cool down. The autoclave contents were transferred to vials, and the catalysts were separated by centrifugation and filtration. For comparison, other alcohols, such as furfuryl alcohol, cyclohexanol, 1-pentanol, 1-butanol, 2-pentanol, 3-butene-1-ol, 1,2-pentanediol (Sinopharm Chemical Regent Co. Ltd., China) were also tested with purities greater than 98%. The recyclability of the K$_2$CO$_3$/ZrO$_2$ catalyst was investigated by reusing the catalyst in four consecutive runs at 130 °C. Prior to each reuse of the catalyst, the reaction crude was allowed to settle down, and the supernatant was removed from the reactor. A fresh charge of reactant was then added to the reactor and the subsequent run was continued.
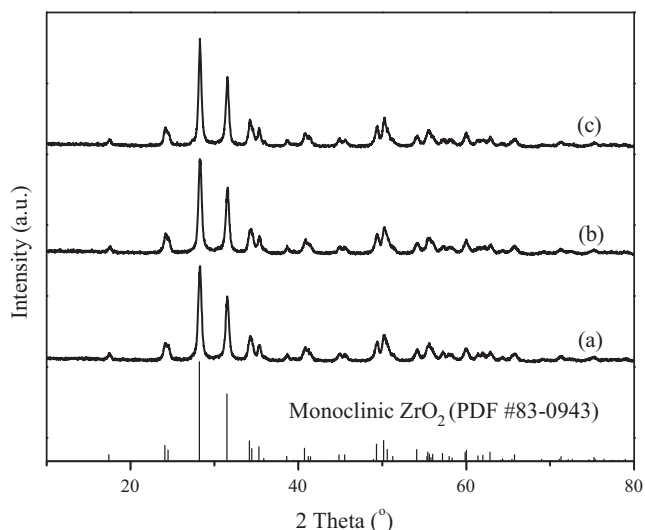
**Fig. 1.** X-ray diffraction patterns of the catalysts: (a) $ZrO_2$; (b) $K_2CO_3/ZrO_2$; (c) $KNO_3/ZrO_2$.



**Fig. 2.** The $CO_2$-TPD profiles for the catalysts: (a) $ZrO_2$; (b) $K_2CO_3/ZrO_2$; (c) $KNO_3/ZrO_2$; (d) Mg–Al-HDT.

The liquid reaction products were analyzed by GC-950 gas chromatograph (Shanghai Haixin chromatogram analysis Co., Ltd, China) equipped with a flame ionization detector (FID) and a capillary column (J&W DB-WAX, $30\,m \times 0.32\,mm$). The conversion and selectivity were determined based on the area normalization method. All the products were identified by GC/MS (GC6890N/5973MSD, Agilent, USA) equipped with a capillary Chromatographic column (J&W DB-WAX: $30\,m \times 0.32\,mm$).

# 3. Results and discussions
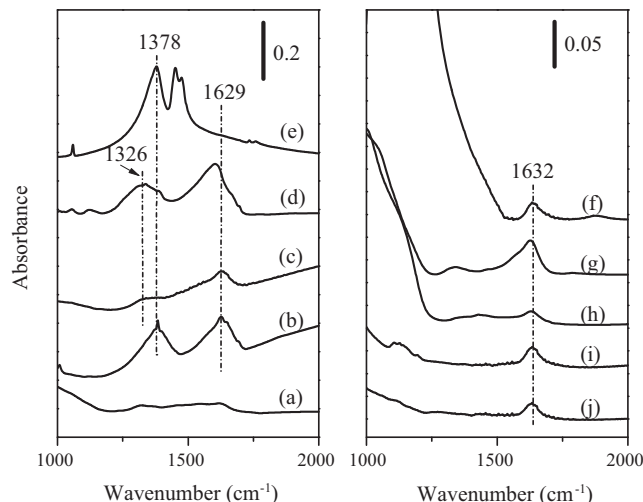
## 3.1. Catalyst characterization

### 3.1.1. XRD patterns

Fig. 1 shows that the $ZrO_2$, $K_2CO_3/ZrO_2$ and $KNO_3/ZrO_2$ obtained after calcinations at $600\,°C$ were well crystalline, and only the diffraction peaks of monoclinic $ZrO_2$ were present. The intensity and position of the peaks were not changed after the impregnation of the potassium salt, which indicated that the bulk structure of the monoclinic $ZrO_2$ was well preserved. The absence of zirconate phase or potassium salt suggested the potassium salt was not located into the lattice of $ZrO_2$ but just interacted with the $ZrO_2$ surface.

### 3.1.2. Textural characterization

Table 1 reports the results of textural characterization of the used typical samples. As can be observed in this table, the $K_2CO_3$ or/and $KNO_3$ incorporation by impregnation method reduced the

**Table 1**
The textural characterization of the catalysts and supports.

| Sample | $S_{BET}$ (m²/g) | Pore volume (cm³/g) | Pore size (nm) |
| --- | --- | --- | --- |
| $K_2CO_3/ZrO_2$ | 19.0 | 0.06 | 12.0 |
| $KNO_3/ZrO_2$ | 14.3 | 0.06 | 12.5 |
| $CsF/\alpha\text{-}Al_2O_3$ | 14.7 | 0.02 | 10.3 |
| $K_2CO_3/\gamma\text{-}Al_2O_3$ | 78.7 | 0.39 | 16.4 |
| MgAl-HDT | 248.3 | 0.54 | 11.7 |
| MgO | 21.4 | 0.04 | 7.8 |
| ZnO | 15.6 | 0.07 | 15.7 |
| $ZrO_2$ | 45.6 | 0.15 | 9.7 |
| $\gamma\text{-}Al_2O_3$ | 197.0 | 0.62 | 9.1 |
| $SiO_2$ | 393.0 | 0.90 | 6.9 |
| $CeO_2$ | 80.3 | 0.23 | 10.9 |

$S_{BET}$ of the $ZrO_2$ based catalysts. Similarly, the $S_{BET}$ of the $K_2CO_3/\gamma$-$Al_2O_3$ catalyst was also significantly lower than the $\gamma$-$Al_2O_3$ support. Therefore, we can conclude that there is a strong interaction between K precursor and the support. The other $CsF/\alpha$-$Al_2O_3$ $K_2CO_3/\gamma$-$Al_2O_3$ MgAl-HDT MgO and ZnO catalysts have different textural properties, but all of them are mainly mesoporous.

### 3.1.3. FT-IR

Fig. 2 is the infrared spectra of different catalysts in the range $800–2000\,cm^{-1}$, which can be assigned to carbonate species or molecular water [26]. The spectrum of $K_2CO_3$ contained three main peaks at 1378, 1451 and $1475\,cm^{-1}$, while the $ZrO_2$ support did not show any prominent peaks. However, two new peaks at 1384 and $1628\,cm^{-1}$ were observed over the $K_2CO_3/ZrO_2$ catalyst, indicating the generation of new carbonate species by the K addition. It can be assigned to carbonate species bonding to the $ZrO_2$ surface. There are seven types of carbonate species which are usually observed upon chemisorptions of $CO_2$ on pure metal oxides: (1) free carbonate with one bond range at $1415–1479\,cm^{-1}$; (2) three bonds originating from momodetate species appearing about 1420–1540, 1330–1390 and $980–1050\,cm^{-1}$; (3) four bands attributed to bidentate species at 1600–1670, 1280–1310, 980–1050 and $830\,cm^{-1}$; (4) four bonds due to bridged species at about 1780–1840, 1250–1280 and $1000\,cm^{-1}$; (5) four bonds originating from biocarbonate species appearing at 1615–1630, 1400–1500 and $1236–1225\,cm^{-1}$ as well as in the hydroxyl region at $3610–3605\,cm^{-1}$; (6) carboxylate species with two bonds at 1570–1630 and $1350–1390\,cm^{-1}$; (7) three bonds belonging to formate species at about 2740–2850, 1580–1620 and $1340–1390\,cm^{-1}$ [27–29]. Accordingly, the carbonate species on the surface of the $K_2CO_3/ZrO_2$ catalyst are assigned to be the carboxylate species (6). These carboxylate species were also observed over the $KNO_3/ZrO_2$ catalyst and the $K_2CO_3/CeO_2$ catalyst. However, the corresponding peaks for the carbonate species were not found on the $K_2CO_3/TiO_2$ (Rutile), $K_2CO_3/TiO_2$(Anatase), $K_2CO_3/\gamma$-$Al_2O_3$ and $K_2CO_3/\alpha$-$Al_2O_3$ catalysts, and the peak at $1632\,cm^{-1}$ was due to the water on the catalyst surface (Fig. 2 B).

### 3.1.4. $CO_2$-thermoprogrammed desorption

Fig. 3 shows the $CO_2$-TPD profiles for the $ZrO_2$, $K_2CO_3/ZrO_2$, $KNO_3/ZrO_2$ and MgAl-catalysts. Pure $ZrO_2$ showed a wide broad shoulder spectrum from 50 to $450\,°C$. The intensity of the peaks was further significantly decreased with the addition of K species
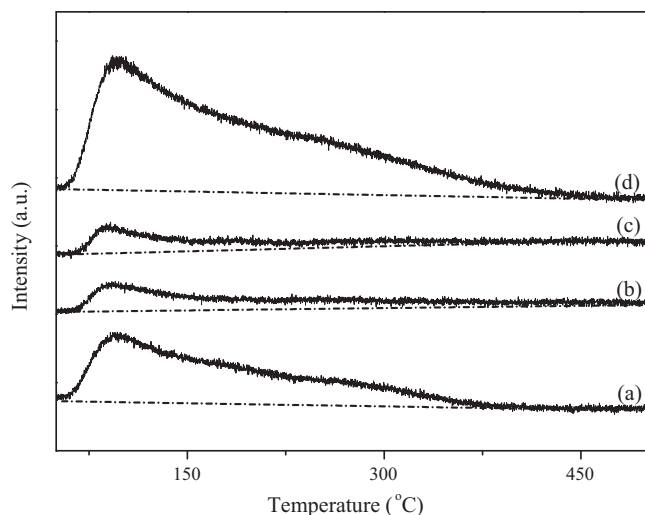
**Fig. 3.** The FTIR of the catalysts: (a) $ZrO_2$; (b) $K_2CO_3/ZrO_2$; (c) $KNO_3/ZrO_2$; (d) $K_2CO_3/CeO_2$; (e) $K_2CO_3$; (f) $K_2CO_3/SiO_2$; (g) $K_2CO_3/TiO_2$ (Rutile); (h) $K_2CO_3/TiO_2$(Anatase); (i) $K_2CO_3/\gamma\text{-}Al_2O_3$; (j) $K_2CO_3/\alpha\text{-}Al_2O_3$.

for the $K_2CO_3/ZrO_2$ and $KNO_3/ZrO_2$ catalyst. The defective oxygen atoms were suggested to be the basic centers on the $ZrO_2$ surface [24], and the FTIR showed that new carboxylate species were generated on the $ZrO_2$ surface after the doping of $K_2CO_3$. Therefore, new carboxylate species were generated from the $K_2CO_3$ that incorporated with the surface basic defective oxygen atoms of the $ZrO_2$. The MgAl-HDT catalyst have a similar broad shoulder $CO_2$ desorption spectrum as $ZrO_2$, but the intensity of the peaks was obviously higher than that of $ZrO_2$. Since the acidic carbon dioxide specially adsorbed on the surface basic sites of the meal oxide surface, there were more strong basic sites over MgAl-HDT catalyst.

### 3.1.5. XPS characterization

XPS analysis was performed on $ZrO_2$ and $K_2CO_3/ZrO_2$ to study the influence of K promotion (Fig. 4). K was detected at a binding energy of 292.5 eV for K $2p_{3/2}$ on the $K_2CO_3/ZrO_2$ catalyst. On both the $ZrO_2$ and $K_2CO_3/ZrO_2$, the binding energy of $Zr3d_{5/2}$ was 182.4 eV, indicating no electronic effect of K on Zr. Hamad et al. reported that there was an electronic enrichment of Zr atom after Cs exchange by forming a Cs–O–Zr bond over the Cs-$ZrO_2$ catalyst, which was due to the homogeneous distribution of $Cs^+$ cations in the $ZrO_2$ material [24]. Here, the K was only located on the surface of $ZrO_2$ over the $K_2CO_3/ZrO_2$ catalyst. Moreover, the carbonate species were increased after the addition of K precursor. Fig. 4 presents the C1s can be decomposed into two components at 284.6 and 288.7 eV. The major one at 284.6 eV was ascribed to adventitious carbon, and the weak shoulder at 288.7 eV was the carbonate species [24,30,31]. The atomic percentage of the carbonate species increased markedly by the addition of $K_2CO_3$, from 8.7% to 25.4%. Furthermore, the asymmetric peaks of O1s XPS spectra were fitted with two symmetrical peaks centered at around 529.9 and 531.5 eV. The major peak at 529.9 eV is corresponding to metal–oxygen–metal bonding [32]. The shoulder peak at high binding energy (531.5–532.7 eV) has been assigned to the defective oxides or oxygen species of the surface carbonates [24,33,34]. The promotion of K resulted in the atomic percentage increasing of the peak at 531.5 eV from 19.4% to 36.2%. As the binding energies of $Zr3d_{5/2}$ and O1s (531.5 eV) were not shifted after K promotion, the shoulder peak at 531.5 eV was the oxygen species of the surface carbonates. Thus, new carbonate species were generated on the $K_2CO_3/ZrO_2$ catalyst.
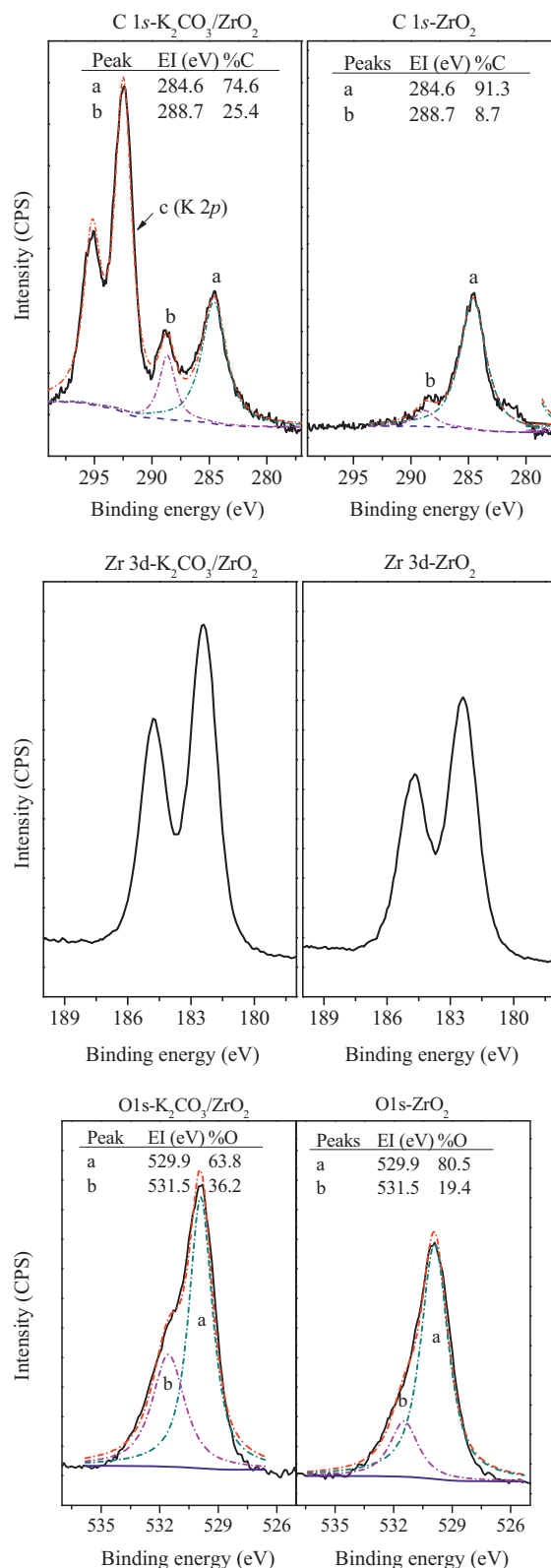


**Fig. 4.** The XPS peaks for $ZrO_2$ and $K_2CO_3/ZrO_2$.

## 3.2. Catalytic transesterification

The catalytic activity of various soluble and solid base catalysts has been directly evaluated in the transesterification of DMC with THFA under solvent-free conditions. The only two products detected were TMC and DTC. Surprisingly, all the catalysts exhibited

**Table 2**
Catalyst results for the transesterification of DMC with tetrahydrofurfuryl alcohol[a]. (The content of K or Cs in the supported catalyst is 1 mmol/$g_{Cat.}$).

| Entry | Catalyst | $t$ (h) | Reaction rate (mmol/$g_{Cat.}$/h) | Conv.(%) | Yield (%) | |
|---|---|---|---|---|---|---|
| | | | | | TMC | DTC |
| 1 | $K_2CO_3/ZrO_2$ | 0.5 | 1974 | 98.7 | 97.7 | 1.0 |
| 2 | $KNO_3/ZrO_2$ | 0.5 | 1966 | 98.3 | 95.9 | 2.4 |
| 3 | MgAl-HDT | 0.5 | 570 | 28.3 | 27.7 | 0.6 |
| 4 | MgO | 0.5 | 43 | 2.1 | 2.1 | 0.0 |
| 5[b] | ZnO[b] | 3.0 | 2 | 6.3 | 6.3 | 0.0 |
| 6[b] | CaO | 3.0 | 23 | 68.9 | 68.1 | 0.8 |
| 7 | $CsF/\alpha-Al_2O_3$ | 0.5 | 75 | 3.7 | 3.7 | 0.0 |
| 8 | $K_2CO_3/CeO_2$ | 0.5 | 1980 | 99.0 | 98.1 | 0.9 |
| 9 | $K_2CO_3/SiO_2$ | 0.5 | 682 | 34.1 | 33.9 | 0.2 |
| 10 | $K_2CO_3/TiO_2$ (Rutile) | 0.5 | 38 | 1.9 | 1.9 | 0.0 |
| 11 | $K_2CO_3/TiO_2$ (Anatase) | 0.5 | 10 | 0.5 | 0.5 | 0.0 |
| 12 | $K_2CO_3/\gamma-Al_2O_3$ | 0.5 | 0 | 0.0 | – | – |
| 13 | $KNO_3/\gamma-Al_2O_3$ | 0.5 | 0 | 0.0 | – | – |
| 14 | $K_2CO_3/\alpha-Al_2O_3$ | 0.5 | 0 | 0.0 | – | – |
| 15 | $K_2CO_3$[c] | 0.5 | – | 98.6 | 97.0 | 1.6 |
| 16 | KOH[d] | 0.5 | – | 98.5 | 97.1 | 1.4 |
| 17 | $ZrO_2$ | 0.5 | 0 | 0.0 | – | – |
| 18 | $CeO_2$ | 0.5 | 0 | 0.0 | – | – |
| 19 | $SiO_2$ | 0.5 | 0 | 0.0 | – | – |
| 20 | Blank | 0.5 | 0 | 0.0 | – | – |

[a] THFA 1.0 g, DMC 29.0 g, Catalyst 0.01 g (1 mmol K/$g_{Cat.}$), 130 °C, closed system in a stainless steel autoclave.

[b] THFA 1.0 g, DMC 29.0 g, Catalyst 0.1 g, 130 °C.

[c] THFA 1.0 g, DMC 29.0 g, $K_2CO_3$ 0.005 mmol, 130 °C.

[d] THFA 1.0 g, DMC 29.0 g, KOH 0.01 mmol, 130 °C.

high selectivity in producing of TMC, despite the large differences in their catalytic activity as shown in Table 2. The $K_2CO_3/ZrO_2$ catalyst exhibited a higher reaction rate (1974 mmol/$g_{Cat.}$/h) than the $CsF/\alpha-Al_2O_3$ catalyst (75 mmol/$g_{Cat.}$/h), which had been reported to be the best catalyst in direct transesterification of diethyl carbonate with THFA [6]. High reaction rate towards the corresponding product was also obtained over the $KNO_3/ZrO_2$ catalyst (1966 mmol/$g_{Cat.}$/h), which have the same amount of potassium (1 mmol/g) as the $K_2CO_3/ZrO_2$ catalyst. Since the support $ZrO_2$ showed no activity in transesterification, the surface species generated by the K precursor-doping might be the key component in the generation of the active sites. Furthermore, the $K_2CO_3$ supported on various supports were investigated. The supported $K_2CO_3/CeO_2$ catalyst produced similar reaction rate as $K_2CO_3/ZrO_2$ catalyst, while the $K_2CO_3/SiO_2$ catalyst displayed moderate yield. Surprisingly, the $K_2CO_3$ supported on $\alpha-Al_2O_3$, $\gamma-Al_2O_3$ and $TiO_2$ (Rutile or Anatase) with the same K content displayed an extremely low reaction rates (<38 mmol/$g_{Cat.}$/h).

The recycling experiment of the catalyst was investigated by taking out the reaction mixture after the reaction completion by using centrifugation, and then a new feed of reactants were added. As reported in Table 3, a marginal decrease of the conversion of THFA from 98.7% to 93.3% suggested stability of the $K_2CO_3/ZrO_2$ catalyst after using four times. Besides, the decreasing selectivity of MTC from 99.0% to 93.5% was due to the generation of the ditetrahydrofurfuryl carbonate (DTC).

The transesterification of DMC with variety of alcohols, including heterocyclic, cyclic, alkyl or alkenyl and diols (Table 3), was studied over the $K_2CO_3/ZrO_2$ catalyst. The corresponding unsymmetrical carbonates were selectively generated from all the monohydric alcohols, and the furan ring or C=C bond was inertness in the transesterification of DMC with alcohols (Table 3, Entries 2 and 7). However, the 1,2-diols led to the formation of cyclic carbonates (Table 3, Entries 8 and 9), which was similar to the transesterification of diethyl carbonate with alcohols over the $CsF/\alpha-Al_2O_3$ catalyst [6]. Although high selectivity of the carbonate was obtained over the $K_2CO_3/ZrO_2$ catalyst, the reaction rates varied with different alcohols. Generally, the reaction rate was increased with the carbon number of the alcohol. For instance, the reaction rate of the transesterification of DMC with n-pentanol was

higher than that with n-butanol (Table 3, Entries 4 and 6). However, the reaction rate of cyclopentanol (C6 alcohol) with substituent on the α-C was lower than that of THFA or n-pentanol (C5 alcohol) without the substituent on the α-C. Similarly, the reaction rate of 2-pentanol (C5 alcohol) was also lower than that of n-butanol (C4 alcohol). Both the carbon number and the electron-donating substituent on the α-C can reduce the acidity of the alcohol. Therefore, the using of lower acidic alcohol as reactant resulted in a higher reaction rate [35].
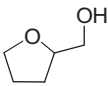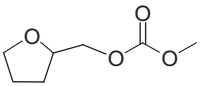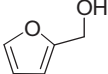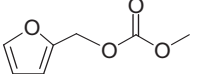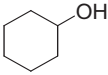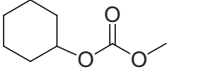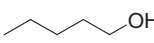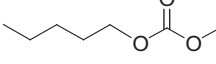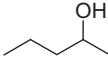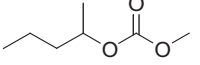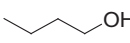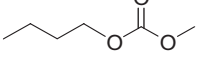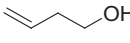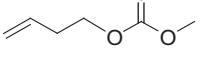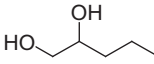
### 3.3. Discussion

The results of transesterification alcohols with DMC indicate that the using of lower acidic alcohol as reactant resulted in a higher reaction rate (Table 3). This agreed with the mechanism of nucleophilic reaction over the basic catalyst. However, the $K_2CO_3/ZrO_2$ catalyst with weaker basicity showed higher reaction rate than the MgAl-HDT catalyst. Veldurthy et al. also found that the total number of basic sites (or the strong basi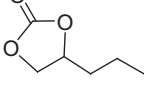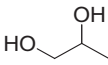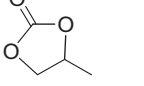c sites) between the reaction rate did not represented a linearity correlation [36]. Therefore, it cannot infer that the basic sites are the only active sites in the transesterification alcohol with DMC over the $K_2CO_3/ZrO_2$ catalyst.

In fact, the $CO_2$-TPD showed that the strong $CO_2$ adsorption sites were almost disappear after the doping of $K_2CO_3$ onto the monoclinic $ZrO_2$ surface. Generally, the $CO_2$ adsorption sites are the terminal hydroxyl groups, $O^{2-}$ centers, and $Zr^{4+}-O^{2-}$ pairs over the monoclinic $ZrO_2$ surface. The stronger basicity is associated to the $Zr^{4+}-O^{2-}$ pairs sites [37]. The FTIR and XPS showed that the carboxylate species was only observed over the $K_2CO_3/ZrO_2$ catalyst, $KNO_3/ZrO_2$ catalyst, and $K_2CO_3/CeO_2$ catalyst, which have correspondingly displayed high reaction rates. Therefore, the surface $Zr^{4+}-O^{2-}$ pairs sites or $O^{2-}$ centers were bonded with the $K_2CO_3$ to form the carboxylate species, which cannot further adsorb the $CO_2$ during TPD experiment.

The equimolar amounts of homogeneous $K_2CO_3$ showed similar high reaction rate as the $K_2CO_3/ZrO_2$ catalyst. However, the stability of the $K_2CO_3/ZrO_2$ catalyst for four times using suggested that the surface carboxylate species cannot be easily leached during the reaction. Therefore, the carboxylate species bonded on the catalyst surface were the active site in transesterification reaction,

**Table 3**
Direct transesterification of DMC with various alcohols over the $K_2CO_3/ZrO_2$ catalyst in solvent-free system[a].

| Entry | Alcohol | Product | Reaction rate (mmol/$g_{Cat}$/h) | Conv. (%) | Sel. (%) |
|---|---|---|---|---|---|
| 1 | | | 1974 | 98.7 | 99.0 |
| | | | 1922 | 96.1[b] | 98.8 |
| | | | 1876 | 93.8[c] | 95.2 |
| | | | 1866 | 93.3[d] | 93.5 |
| 2 | | | 1818 | 90.9 | 95.9 |
| 3 | | | 1552 | 77.6 | 99.0 |
| 4 | | | 1900 | 95.0 | 99.7 |
| 5 | | | 512 | 25.6 | 100.0 |
| 6 | | | 728 | 36.4 | 99.9 |
| 7 | | | 574 | 28.7 | 99.4 |
| 8 | | | 1968 | 98.4 | 100.0 |
| 9 | | | 2000 | 100.0 | 100.0 |

[a] THFA 1.0 g, DMC 29.0 g, Catalyst 0.01 g, 130 °C, 0.5 h.
[b] Second cycle.
[c] Third cycle.
[d] Fourth cycle.
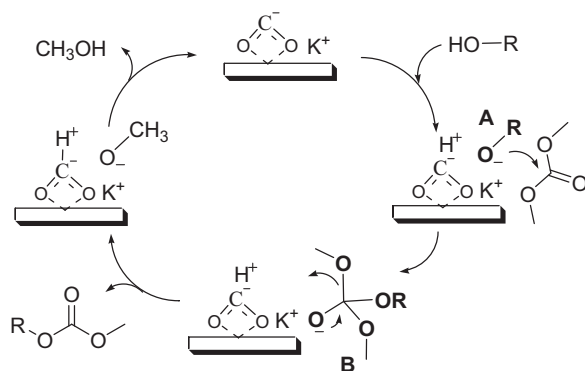


**Scheme 2.** The $K_2CO_3/ZrO_2$ catalyzed transesterification mechanism.

which can explain the high activity of the $K_2CO_3/ZrO_2$ catalyst, the $KNO_3/ZrO_2$ catalyst, and the $K_2CO_3/CeO_2$ catalyst. According to our previous work, the basic precursor might neutralize with the surface acid sites to form a neutral or inactive surface after calcination [38]. Thus, the $\alpha$-$Al_2O_3$, $\gamma$-$Al_2O_3$ and $TiO_2$ (Rutile or Anatase) catalysts combined with the $K_2CO_3$ cannot form the carboxylate species but might be an inactive surface, which resulted in the low catalytic activity.

According to the mechanism of the transesterification over the $CsF/\alpha$-$Al_2O_3$ [6], a similar mechanism is proposed as shown in

Scheme 2. The reaction is catalyzed by the carboxylate species bonded on the $ZrO_2$ surface. The catalytic cycle may be initiated by abstraction of a proton by a negatively changed carbon of the carboxylate species from an alcohol to generate an alkoxide anion stabilized by $K^+$ ions. The K-alkoxide (Scheme 2, A) can then react with DMC by forming the tetrahedral intermediate (Scheme 2, B) to yield unsymmetrical alkyl carbonate and methanol. Veldurthy et al. suggested that the Cs-alkoxides constitute weakly coordinated species and enhance the nucleophilicity, resulting in higher reaction rate [6]. This idea is also suited for the mechanism on the carboxylate species, which adsorbs the acidic $CO_2$ weakly.

## 4. Conclusion

The $K_2CO_3/ZrO_2$ catalyst is an efficient and reusable catalyst for the selective synthesis unsymmetrical organic carbonates including the THFA carbonate. The carboxylate species, generated from the interaction between the $K_2CO_3$ and the $ZrO_2$ support, is firstly confirmed to be the active site in the solvent free transesterification reaction. Correspondingly, no such carboxylate species are generated over the catalysts of $K_2CO_3$ supported on $\alpha$-$Al_2O_3$, $\gamma$-$Al_2O_3$ or $TiO_2$ (Rutile or Anatase), which show a rather low activity in the catalytic process. These results are important to understand the mechanism for the transesterification of DMC with biomass-derived alcohol compounds, and provide guidance for the design of new catalytic formulations.

## Acknowledgments

## References

[1] G.W. Huber, S. Iborra, A. Corma, Chem. Rev. 106 (2006) 4044–4098.
[2] A. Corma, S. Iborra, A. Velty, Chem. Rev. 107 (2007) 2411–2502.
[3] T. Sakakura, J.-C. Choi, H. Yasuda, Chem. Rev.—Columbus 107 (2007) 2365–2387.
[4] T. Sakakura, K. Kohno, Chem. Commun. (2009) 1312–1330.
[5] S.-c. Kinoshita, M. Kotato, Y. Sakata, M. Ue, Y. Watanabe, H. Morimoto, S.-i. Tobishima, J. Power Sources 183 (2008) 755–760.
[6] B. Veldurthy, J.-M. Clacens, F. Figueras, Eur. J. Org. Chem. 2005 (2005) 1972–1976.
[7] A. Takagaki, K. Iwatani, S. Nishimura, K. Ebitani, Green Chem. 12 (2010) 578–581.
[8] D. Darensbourg, S.J. Wilson, Green Chem. 14 (2012) 2665–2671.
[9] Y. Ono, Catal. Today 35 (1997) 15–25.
[10] J.-Q. Wang, J. Sun, C.-Y. Shi, W.-G. Cheng, X.-P. Zhang, S.-J. Zhang, Green Chem. 13 (2011) 3213–3217.
[11] P. Tundo, M. Selva, Acc. Chem. Res. 35 (2002) 706–716.
[12] L.E. Schniepp, H.H. Geller, J. Am. Chem. Soc. 68 (1946) 1646–1648.
[13] S. Koso, I. Furikado, A. Shimao, T. Miyazawa, K. Kunimori, K. Tomishige, Chem. Commun. (2009) 2035–2037.
[14] N. Tatsuya, Daicel Chem. Ind. Ltd., JP 0407035, 1992.
[15] F. Nobuo, O. Fumiol, Tetsuo, F.Takahito, Idemitsu Kosan Co., JP 08239347, 1996.
[16] M.Inaba, K.Sawa and T.Tanaka, Mitsubishi Chem. Co., JP 09110805, 1997.
[17] T. Fujii, T. Ishibashi, N. Fujikawa, Idemitsu Kosan Co., JP 09169703 1997.
[18] Z.-h. Fu, Y. Ono, J. Mol. Catal. A: Chem. 118 (1997) 293–299.
[19] W.B. Kim, J.S. Lee, J. Catal. 185 (1999) 307–313.
[20] Z. Weiqing, Z. Xinqiang, W. Yanji, Z. Jiyan, Appl. Catal., A 260 (2004) 19–24.
[21] M. Fuming, P. Zhi, L. Guangxing, Org. Process Res. Dev. 8 (2004) 372–375.
[22] R. Bai, Y. Wang, S. Wang, F. Mei, T. Li, G. Li, Fuel Process. Technol. 106 (2013) 209–214.
[23] I. Zielinska-Nadolska, K. Warmuzinski, J. Richter, Catal. Today 114 (2006) 226–230.
[24] B. Hamad, A. Perard, F. Figueras, F. Rataboul, S. Prakash, N. Essayem, J. Catal. 269 (2010) 1–4.
[25] M. Fan, P. Zhang, Energy Fuels 21 (2007) 633–635.
[26] K. Pokrovski, K.T. Jung, A.T. Bell, Langmuir 17 (2001) 4297–4303.
[27] G. Busca, V. Lorenzelli, Mater. Chem. 7 (1982) 89–126.
[28] A.M. Turek, I.E. Wachs, E. DeCanio, J. Phys. Chem. 96 (1992) 5000–5007.
[29] V.F. Kiselev, V. Krylov, Adsorption and catalysis on transition metals and their oxides, in: G. Ertl, R. Gomer (Eds.), Springer Series in Surface Sciences, 9, Springer-Verlag, Berlin, 1989.
[30] S.-J. Xiao, M. Textor, N.D. Spencer, H. Sigrist, Langmuir 14 (1998) 5507–5516.
[31] X.-Y. Zhang, H.-P. Li, X.-L. Cui, Y. Lin, J. Mater. Chem. 20 (2010) 2801–2806.
[32] Navío, Hidalgo, G. Colón, S.G. Botta, M.I. Litter, Langmuir 17 (2000) 202–210.
[33] X. Tang, Y. Li, X. Huang, Y. Xu, H. Zhu, J. Wang, W. Shen, Appl. Catal., B 62 (2006) 265–273.
[34] M.-S. Fan, A.Z. Abdullah, S. Bhatia, Appl. Catal., B 100 (2010) 365–377.
[35] F.A. Carey, R.J. Sundberg, Advanced Organic Chemistry: Part A: Structure and Mechanisms, Springer, 2007.
[36] B. Veldurthy, J.-M. Clacens, F. Figueras, J. Catal. 229 (2005) 237–242.
[37] B. Bachiller-Baeza, I. Rodriguez-Ramos, A. Guerrero-Ruiz, Langmuir 14 (1998) 3556–3564.
[38] B. Zhang, Y. Zhu, G. Ding, H. Zheng, Y. Li, Appl. Catal., A 443–444 (2012) 191–201.

# Update

## Applied Catalysis B: Environmental

Corrigendum

# Corrigendum to "Transesterification of dimethyl carbonate with tetrahydrofurfuryl alcohol on the $K_2CO_3/ZrO_2$ catalyst—Function of the surface carboxylate species" [Appl. Catal. B: Environ. 152–153 (2014), 226–232]

Bin Zhang [a], Guoqiang Ding [b], Hongyan Zheng [b], Yulei Zhu [a,b,*]

[a] State Key Laboratory of Coal Conversion, Institute of Coal Chemistry, Chinese Academy of Sciences, P.O. Box 165, Taiyuan 030001, PR China
[b] Synfuels CHINA Co., Ltd., Taiyuan 030032, PR China

Author would like to apologize for the inconvenience caused.

The authors regret to inform that the caption of Fig. 2 and Fig. 3 are reversed in this paper.

**In page 228, right column, the caption of** Fig. 2 **should be replaced by** "The FTIR of the catalysts: (a) $ZrO_2$; (b) $K_2CO_3/ZrO_2$; (c) $KNO_3/ZrO_2$; (d) $K_2CO_3/CeO_2$; (e) $K_2CO_3$; (f) $K_2CO_3/SiO_2$; (g) $K_2CO_3/TiO_2$ (Rutile); (h) $K_2CO_3/TiO_2$(Anatase); (i) $K_2CO_3/\gamma$- $Al_2O_3$; (j) $K_2CO_3/\alpha$-$Al_2O_3$".

**In page 229, left column, the caption of** Fig. 3 **should be replaced by** "The $CO_2$-TPD profiles of the catalysts: (a) $ZrO_2$; (b) $K_2CO_3/ZrO_2$; (c) $KNO_3/ZrO_2$; (d) MgAl- HDT".